Science of the Total Environment 818 (2022) 151722

Contents lists available at ScienceDirect

Science of the Total Environment

journal homepage: www.elsevier.com/locate/scitotenv

Unveiling the dipole synergic effect of biogenic and anthropogenic emissions on ozone concentrations

Yang Gao [a,*], Feifan Yan [a], Mingchen Ma [a], Aijun Ding [b], Hong Liao [c], Shuxiao Wang [d], Xuemei Wang [e], Bin Zhao [d], Wenju Cai [f,g], Hang Su [h,i], Xiaohong Yao [a], Huiwang Gao [a]

[a] Key Laboratory of Marine Environment and Ecology, and Frontiers Science Center for Deep Ocean Multispheres and Earth System, Ministry of Education, Ocean University of China, and Qingdao National Laboratory for Marine Science and Technology, Qingdao 266100, China
[b] Joint International Research Laboratory of Atmospheric and Earth System Sciences, School of Atmospheric Sciences, Nanjing University, Nanjing, China
[c] Jiangsu Key Laboratory of Atmospheric Environment Monitoring and Pollution Control, Jiangsu Collaborative Innovation Center of Atmospheric Environment and Equipment Technology, School of Environmental Science and Engineering, Nanjing University of Information Science & Technology, Nanjing 210044, China
[d] State Key Joint Laboratory of Environment Simulation and Pollution Control, School of Environment, Tsinghua University, Beijing 100084, China
[e] Institute for Environmental and Climate Research, Jinan University, Guangzhou 510000, China
[f] Physical Oceanography Laboratory/CIMST, Ocean University of China and Qingdao National Laboratory for Marine Science and Technology, Qingdao 266100, China
[g] CSIRO Marine and Atmospheric Research, Aspendale, Victoria 3195, Australia
[h] Multiphase Chemistry Department, Max Planck Institute for Chemistry, Mainz D-55128, Germany
[i] State Environmental Protection Key Laboratory of Formation and Prevention of Urban Air Pollution Complex, Shanghai Academy of Environmental Sciences, Shanghai 200233, China

HIGHLIGHTS

- Almost 500 numerical experiments by perturbing anthropogenic emissions were designed.
- The synergic effect of biogenic and anthropogenic emissions on ozone is examined.
- We found more enhanced role of biogenic emissions in the ozone formation in future.

GRAPHICAL ABSTRACT

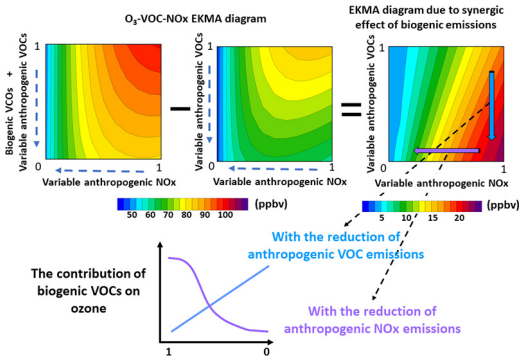

ARTICLE INFO

Article history:
Received 10 September 2021
Received in revised form 4 November 2021
Accepted 12 November 2021
Available online 20 November 2021

Editor: Pavlos Kassomenos

Keywords:
Biogenic emissions
EKMA diagram
Controllable biogenically induced ozone
SSP

ABSTRACT

Biogenic emissions are widely known as important precursors of ozone, yet there is potentially a strong interaction and synergy between biogenic and anthropogenic emissions, including volatile organic compounds (VOCs) and nitrogen oxides (NOx), in modulating ozone formation. To a large extent, the synergy affects the effectiveness of anthropogenic emission control, thereby reshaping the O_3-NOx-VOC empirical kinetic modeling approach (EKMA) diagram. Focusing on the ozone pollution period of June 2017 in the North China Plain, we design almost 500 numerical experiments using regional air quality model Community Multiscale Air Quality (CMAQ) that revealed an interesting synergic effect, defined as the contribution of biogenic emissions to ozone concentrations concomitant with a reduction in anthropogenic emissions. A quasi-EKMA diagram is constructed to delineate the contribution of biogenic emissions to ozone concentrations, indicative of a linearly amplified or nonlinearly weakened result associated with reductions in anthropogenic VOCs or NOx emissions, respectively, illustrating the dipole characteristics of the synergic effect. The reduced ozone contribution from biogenic emissions along with NOx emission reduction can be used to represent controllable biogenically induced ozone (BIO). Both the amplified and controllable BIO are tightly linked to both local emissions and regional transport,

* Corresponding author.
E-mail address: yanggao@ouc.edu.cn (Y. Gao).

https://doi.org/10.1016/j.scitotenv.2021.151722

implicative of an essential role in joint regional emission control. In regard to ozone exceedance, the role of biogenic emissions may be even more important, in that its contribution is comparable to or even larger than that of anthropogenic emissions when associated with a reduction in anthropogenic emissions, which is clearly demonstrated based on the near carbon neutrality scenario shared socioeconomic pathway (SSP) 126. Meanwhile, the biogenic emissions may steer the modulation of anthropogenic emissions in the change rate of MDA8 ozone concentration. Therefore, the synergic effect of biogenic and anthropogenic emissions elucidated in this study should be carefully considered in future ozone pollution control.

1. Introduction

Biogenic emissions are important precursors of ozone, and quantification of their impact on ozone concentration, primarily through numerical sensitivity experiments, demonstrates that biogenic emissions contribute substantially to ozone accumulation (Li et al., 2018; Wu et al., 2020). For example, the regional air quality modeling results in Wu et al. (2020) revealed as large as 47 μg m^{-3} of ozone enhancement in eastern and southwestern China in July 2017 due to biogenic volatile organic compound (VOC) emissions.

In addition to biogenic emissions, the effect of anthropogenic VOC and nitrogen oxides (NOx) emissions on ozone formation has been well established in particular through the examination of O_3-NOx-VOC relationship based on the empirical kinetic modeling approach (EKMA) diagram and identification of VOC-limited or NOx-limited regimes (Sillman, 1999; Sillman and He, 2002; Ou et al., 2016). Specifically, based on the ratio of formaldehyde (HCHO) to NO_2, Wang et al. (2021) found VOC-limited regime tending to occur in urban areas of China, and further indicated that the changes in anthropogenic emissions such as NOx may steer the shift from VOC-limited regime to NOx-limited regime from 2016 to 2019.

The role of biogenic emissions in affecting the ozone concentration may be modulated by the changes in anthropogenic emissions. For instance, Tao et al. (2003) conducted sensitivity simulations by comparing two scenarios, one with biogenic emissions only and the other one with both anthropogenic and biogenic emissions, and found strong synergy between anthropogenic and biogenic emissions across the US. By further applying the factor separation (FS) technique, originally proposed by Stein and Alpert (1993) to elucidate the factors affecting atmospheric circulation, they found that a large portion of biogenic contributions to ozone was influenced by anthropogenic emission sources, indicating that biogenic effects can be mediated through the control of anthropogenic emissions. Recently, Li et al. (2018) conducted simulations applying the FS technique in four scenarios, including cases with both anthropogenic and biogenic emissions, anthropogenic emissions only, biogenic emissions only and neither type of emissions. The results indicated that the synergy between anthropogenic and biogenic emissions was of vital importance, with a magnitude even comparable to the effect of anthropogenic emissions over some locations in the Guanzhong Basin, China.

The interaction between biogenic and anthropogenic emissions has been examined more comprehensively in relation to the influence of biogenic emissions on secondary organic aerosol (SOA) formation (Carlton et al., 2010; Xu et al., 2015; Wu et al., 2020). Based on observational data, Xu et al. (2015) found that levels of biogenic SOA derived from isoprene in the southeastern United States may be affected by anthropogenic emissions, such as SO_2, through the modulation of sulfate as well as the subsequent uptake of epoxydiols (IEPOX). Combining 22 numerical simulations over the United States based on a regional air quality model from August 15 to September 4, 2003, Carlton et al. (2010) found that decrease in anthropogenic emissions may induce a reduction of more than 50% in biogenic SOA in the eastern United States. This could possibly be attributed to the decrease in SOA condensation and implied a strong interaction between anthropogenic and biogenic emissions, suggesting that biogenic SOA formation might be controlled.

The synergic effect of biogenic emissions on ozone formation, however, has not been systematically investigated so far. Particularly in situations with gradually tightened controls of anthropogenic emissions, i.e., in the scenarios of Coupled Model Intercomparison Project Phase 6 (CMIP6) shared socioeconomic pathway (SSPs; (Rao et al., 2017; Riahi et al., 2017)) and carbon neutrality in China (Cai et al., 2021), the interactions between biogenic and anthropogenic emissions may even reshape the O_3-NOx-VOC relationship in EKMA diagram. To examine the synergic effect, the period of June 2017 over the North China Plain (NCP) was selected due to the severe and persistent ozone pollution during this period (Ma et al., 2019; Yan et al., 2021) resulting from heat waves and stagnant weather conditions that are conducive to ozone formation and accumulation (Gao et al., 2013; Zhang et al., 2018b; Gao et al., 2020b). The NCP region was selected primarily because it was prone to ozone pollution, which had been well acknowledged in a number of studies (Li et al., 2019; Lu et al., 2019; Shen et al., 2020). Mimicking the O_3-NOx-VOC EKMA diagram, this study aims to thoroughly elucidate the synergic effect of biogenic and anthropogenic emissions through the construction of a quasi EKMA diagram in the context of anthropogenic emission control, and potentially provide guidance to alleviate ozone exceedance.

2. Model configurations and scenario designs

The coupled Weather Research and Forecasting (WRF; version 3.8) and Community Multiscale Air Quality (CMAQ; version 5.2) model is used to conduct the simulations, and model configurations are the same as those in our previous studies (Ma et al., 2019; Gao et al., 2020a; Yan et al., 2021). The simulation domain covers China and a few other areas (Fig. 1), with the region of NCP (red square in Fig. 1) as one of the major focuses in this study. In brief, Carbon Bond version 6 (CB6) is used as the gas chemistry mechanism, and Aerosol Module Version 6 (AERO6) is used to model the aerosol processes in CMAQ. The initial and boundary conditions are from the NCEP Climate Forecast System Reanalysis (CFSR) version 2 (Saha et al., 2014) for WRF simulations and from the Model for Ozone and Related chemical Tracers, version 4 (MOZART-4; (Emmons et al., 2010)) for CMAQ simulations. The emission inventory is the same as that detailed in Yan et al. (2021). The spatial resolution is 36 km by 36 km, and the simulation starts approximately one week prior to June 1 2017 as spin up, with the analysis focusing on June 1 to June 30, 2017.

Considering the primary ozone precursors of VOCs and NOx, as well as the O_3-NOx-VOC EKMA diagram, four groups of scenarios are designed by perturbing the anthropogenic VOC and NOx emissions (Table 1), with each group including eleven by eleven cases, totaling 121 scenarios. To identify the synergic effect of biogenic and anthropogenic emissions, biogenic emissions are only included in groups ① and ③. Anthropogenic emission reduction is applied over either the NCP (groups ① and ②) or the entire domain (groups ③ and ④) to isolate the effect of regional transport on ozone pollution in the NCP. The

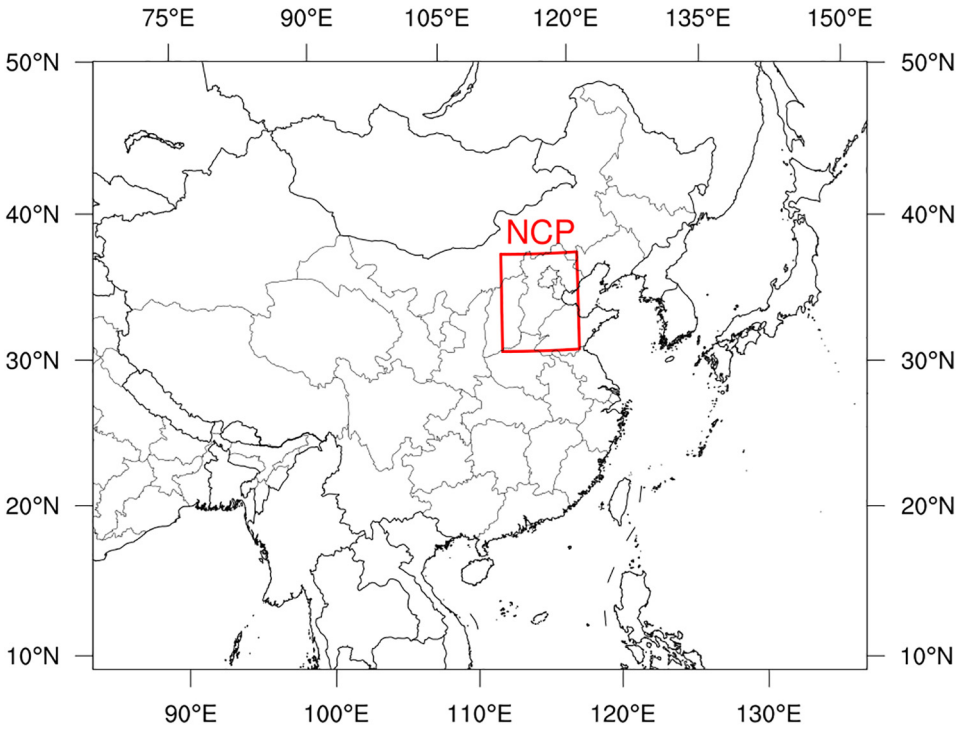

Fig. 1. The simulation domain with the region of North China Plain (NCP; red square).

simulated results including all anthropogenic (without reduction) and biogenic emissions are compared with observations in our previous study (Fig. 2c in Yan et al. (2021)), showing relatively low bias of −8% for maximum daily 8-hr average (MDA8) ozone over NCP, warranting high confidence in interpreting the model results. Furthermore, the findings discussed in the following sections should not be affected by the bias considering they are largely compared between the numerical sensitivity experiments with the basis scenario.

The simulation period is fixed in June 2017, and the analysis focuses on either the entire month or high ozone episodes (June 14–21, June 26–30). The selection of the episode is based on the previous study (Ma et al., 2019), with the criteria set as the long-lasting ozone events in the upper range of class III (82–110 ppbv). The MDA8 ozone concentration averaged over urban Beijing or NCP is focused on for the analysis below, whereas the emission reduction is operated on either NCP or the entire domain.

To estimate the possible changes in future ozone concentrations assuming comparable weather conditions, the new generation of emission projection designed in CMIP6 SSPs (Kriegler et al., 2012) are applied in this study. Compared to the previous scenarios such as Representative Concentration Pathways (RCPs; (van Vuuren et al., 2011)) which does not take into account the socioeconomic narratives, there are five different socio-economic conditions for global futures in regard of climate change adaptation and mitigation in SSPs (SSP1-5; (Rao et al., 2017; Riahi et al., 2017)). Please note that emissions may increase particularly during 2020–2040 in SSP2 or SSP5 (i.e., Supplementary Table 1) partly due to delays in global cooperation with regions (Rao et al., 2017; Gidden et al., 2019).

Table 1
The emission control scenarios designed in this study.

	Anthropogenic emissions		Biogenic emissions
	VOCs emissions	NOx emissions	
①	0–100%[a]	0–100%[a]	On
②	0–100%[a]	0–100%[a]	Off
③	0–100%[b]	0–100%[b]	On
④	0–100%[b]	0–100%[b]	Off

[a] 10% interval from 0 to 100% emission reduction over the NCP.
[b] 10% interval from 0 to 100% emission reduction over the entire domain.

3. Results and discussions

To elucidate the effectiveness of emission reductions on ozone pollution in urban Beijing, we show in Fig. 2 the EKMA diagram that illustrates MDA8 ozone concentrations as emissions of VOCs and NOx are reduced over the NCP area (scenarios ① and ② listed in Table 1). When including both anthropogenic and biogenic emissions, the monthly mean MDA8 ozone concentration in urban Beijing is 84 ppbv (top right grid (corner) in Fig. 2a). The EKMA diagram reflects the transition from VOC-limited to NOx-limited regimes as NOx emissions are reduced, i.e., it shows that the ozone concentration increases when NOx emissions start to decrease and then decreases once NOx emissions are further reduced. A comparable EKMA diagram is created by eliminating biogenic emissions in Fig. 2b, although it has smaller magnitude of ozone concentrations and a left shift of the ozone peak (Fig. 2b vs. Fig. 2a) due to the decrease in VOC emissions. The effect of biogenic emissions on MDA8 ozone concentrations associated with reduction in anthropogenic emissions (Fig. 2c), calculated based on the subtraction of the results shown in Fig. 2b from those in Fig. 2a, is defined in this study as the synergic effect. Interestingly, the synergic effect is enhanced with the reduction of anthropogenic VOCs, whereas the opposite pattern is observed with the reduction of anthropogenic NOx emissions.

The mean monthly synergic effect over urban Beijing ranges from 2.1 ppbv to 12.0 ppbv (Fig. 2c). The features exhibited in the ozone variations during the high ozone episodes (June 14–21, June 26–30; Fig. 2d–f) closely mimic those displayed in the monthly data despite a weaker titration effect due to stronger photochemical reactions, with a somewhat larger synergic effect, ranging from 3.4 ppbv to 18.6 ppbv.

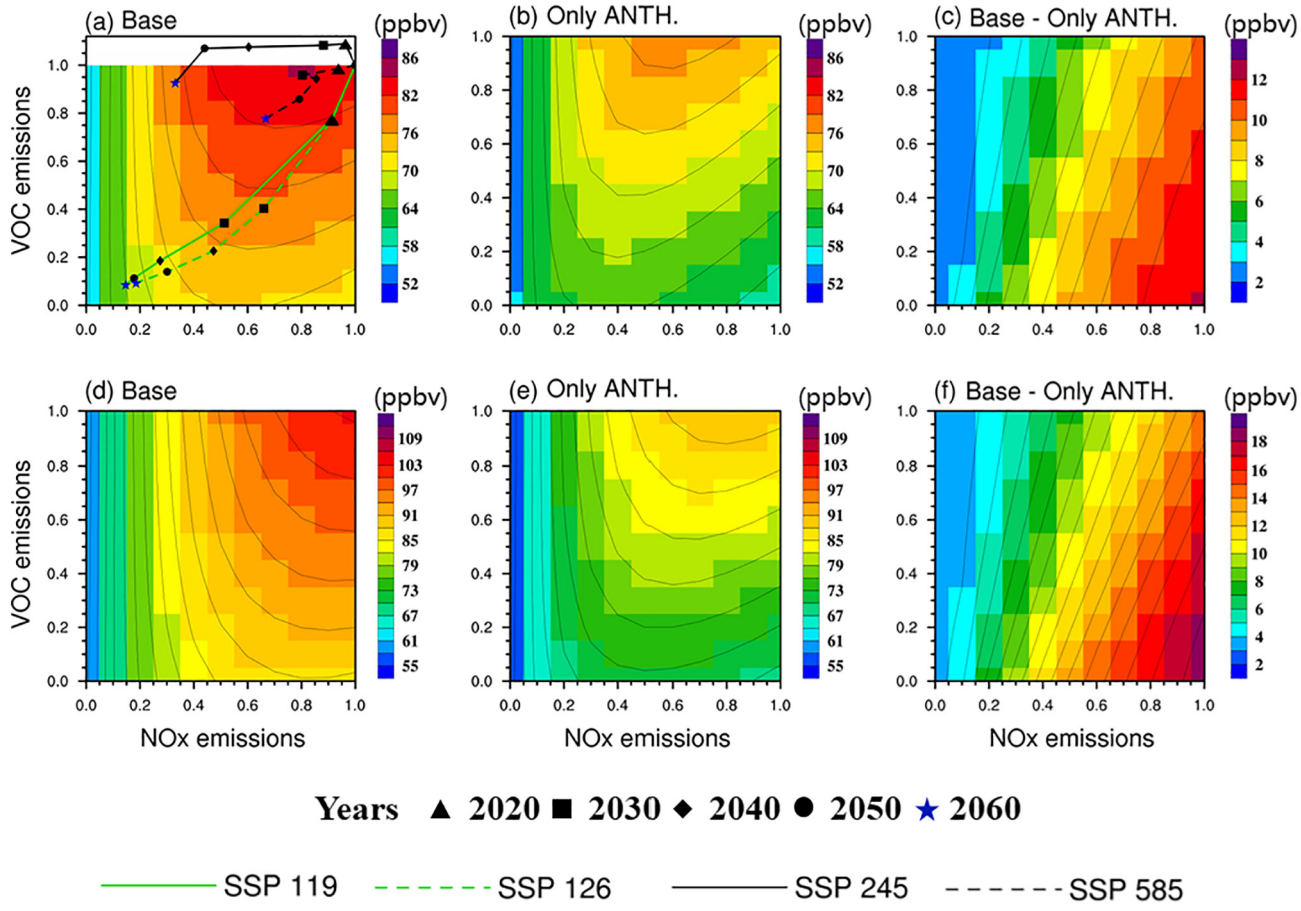

Fig. 2. The EKMA diagram of MDA8 ozone concentrations over urban Beijing. The MDA8 ozone is averaged over the month of June (top) and the episodic events (June 14–June 21, June 26–June 30; bottom), as emissions are reduced over the NCP. Shown are cases with both anthropogenic and biogenic emissions (left column), anthropogenic emissions only (middle column) and the biogenic emissions only (right column: differences between the left and middle columns). The numbers on the X and Y axes indicate the ratio of anthropogenic emissions in different sensitivity cases, and the value 1.0 represents the case without the respective emission (VOCs or NOx) change and 0.0 means the respective emissions (VOCs or NOx) are zeroed out. The markers and connecting lines in panel (a) show the emission changes relative to June 2015 over the NCP every 10 years during 2020–2060, under the four SSP pathways.

Compared with those in urban Beijing (Fig. 2), the variations in MDA8 ozone concentrations over the NCP region (Supplementary Fig. 1) under the same emission reductions show generally similar characteristics, with a clearly discernible diminished titration effect. With emission reductions over the entire domain, the variations in MDA8 ozone concentrations over urban Beijing (Supplementary Fig. 2) and the NCP (Supplementary Fig. 3) are also comparable.

To estimate the possible changes in future ozone concentrations, four emission pathways in SSPs, including SSP119, 126, 245 and 585, are delineated with markers and lines in Fig. 2a. Please note that the emission baseline is calculated over the NCP in June 2015, and the emission change rate is then achieved using the baseline emission divided by the emissions in June of each 10-year interval from 2020 to 2060, when carbon neutrality is scheduled to be achieved in China; the long-term emission variation trends are generally consistent on monthly and annual scales. The markers reflecting reduced emissions in SSPs are used to estimate the corresponding MDA8 ozone concentration in urban Beijing under the same respective conditions, which can be used to infer what ozone concentration might be in the future assuming invariable meteorological conditions. Please note that anthropogenic emissions in China are projected to decrease in three of the four SSP projections mentioned above, except SSP245, where emissions in the near future are projected to increase instead (Fig. 2a). SSP126 is quite close to the mission of carbon neutrality in terms of both CO_2 (Cai et al., 2021) and air pollutant emission pathways, although an alternative intermediate case between SSP 119 and 126 could be designed based on Cheng et al. (2021). There is an apparent decrease in ozone concentrations in most of the SSP scenarios, with the lowest concentrations of 69.4 ppbv and 76.6 ppbv occurring in SSP126 in 2060 as averaged in June (Fig. 2a) and during the ozone episodic events (Fig. 2b), respectively.

One question we ask is at what ratio the reduction in anthropogenic VOC to NOx emissions may yield the optimal effect, i.e., the fastest rate in ozone concentration decrease per unit change of emissions. In Fig. 3, different reduction ratios of VOC to NOx emissions are selected to illustrate their modulation of ozone, and the 1:1 ratio can be considered the separation line (black dashed line). Dots located in the same column represent fixed NOx emission reduction rate and show that larger reduction of VOC emissions corresponds to lower MDA8 ozone concentrations, consistent with the discussions above. Similarly, the cyan dots located on the Y axis indicate that without NOx emission changes, the mean MDA8 ozone concentration in urban Beijing decreases linearly along with the reduction in VOC emissions. The monthly mean MDA8 ozone concentration in June 2017 including all anthropogenic and biogenic emissions shows an increase at the beginning particularly when only NOx emissions are reduced (red dots in Fig. 3a), indicative of the effect of NO titration (Gao et al., 2013) and ozone production inhibition (Romer et al., 2018), which is more obvious when only anthropogenic emissions are included (Fig. 3b). The titration effect also leads to a situation in which the decrease in VOC emissions alone is even more effective in reducing MDA8 ozone concentration than the simultaneous decrease in VOC and NOx emissions at the same rate until the VOC emission reduction reaches a fairly large amount around 70% (cyan dots vs.

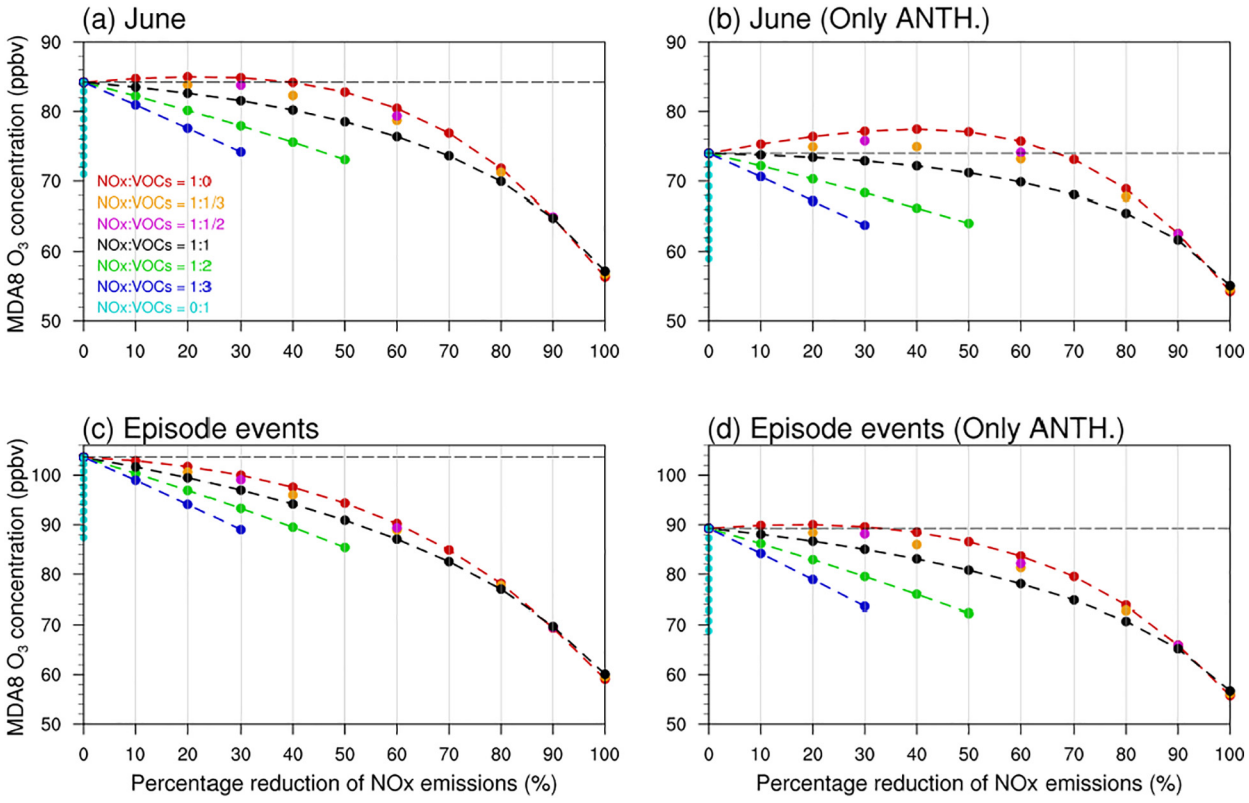

Fig. 3. MDA8 ozone concentration change rate over urban Beijing. Shown are results during June 2017 (top) and the ozone episode (June 14–June 21, June 26–June 30; bottom) under different reduction ratios of anthropogenic NOx to VOC emissions, with both anthropogenic and biogenic emissions included (left column) or anthropogenic emissions only (right column) included. The X axis implies the percentage reduction in NOx emissions, and the reduction in VOCs can be inferred based on the ratio of NOx to VOCs (listed in the top left panel). The ratio of NOx to VOCs at 1:0 means no emission reduction of VOCs (red dots), while 0:1 means no emission reduction of NOx (cyan dots in Y axis). The dashed gray line parallel to X axis is used to demarcate the MDA8 ozone values above which indicative of the effect of NO titration.

black dots in Fig. 3a, b, d). Note there is an exception with biogenic emissions included during the episode when stronger photochemical reactions occur (cyan dots vs. black dots in Fig. 3c), stressing the important role of biogenic emissions in steering the modulation of anthropogenic emission reduction on the change rate of MDA8 ozone concentration. Another unique feature is the convergence as NOx emissions are reduced, meaning that when NOx is reduced to a large extent, the concurrent reductions of NOx and VOC emissions yield almost the same effect as the reduction of NOx emissions alone (i.e., red dots vs. black dots in Fig. 3); this result highlights the essential role that NOx emissions have in ozone modulation and the dramatic efficacy of a greater reduction in NOx emissions.

Below the 1:1 ratio reduction line (dashed black), the larger reduction of VOC relative to NOx emissions generally lies in the lower flank of MDA8 ozone concentrations (i.e., green vs. blue lines in Fig. 3) when their total percentage reduction of VOCs and NOx are the same, implying a faster MDA8 ozone decrease rate with larger VOC to NOx emission ratio. Above the 1:1 line, due to the existence of NO titration and ozone production inhibition, the larger ratio of NOx to VOC emissions triggers a faster ozone decrease when the emission reduction particularly of NOx reaches a relatively larger amount to potentially shift the regime from VOC-limited to NOx-limited one. If the same total percentage of emissions is reduced, VOC emissions only seem to be the most efficient, followed by larger reduction rate of VOC to NOx emissions or NOx to VOC emissions. A comparable conclusion was drawn based on close to 40 numerical simulation cases, illustrating that the most effective way in reducing the maximum hourly ozone is the VOC only reduction, followed by a reduction ratio of VOCs to NOx at 3:1, 2:1 and 1:1 in the manufacturing city of Foshan located in the Pearl River Delta (PRD) region, China (Chen et al., 2019).

To investigate the possible nonlinear behavior of the synergic effect of biogenic emissions, Fig. 4 shows the evolution of MDA8 ozone concentrations in urban Beijing contributed by biogenic emissions under selected scenarios of anthropogenic VOC and NOx emission control over the NCP during June (top) and episodic events (bottom) and depicts a couple of unique features. As anthropogenic VOC emissions are reduced by intervals of 10% from 1.0 (no reduction) to 0.0 (100% reduction) under a fixed amount of NOx emissions, the MDA8 ozone concentration contributed by biogenic emissions shows a linearly monotonic increase with a correlation coefficient of almost 1.0, implicative of an amplified synergic effect (Fig. 4a). It is interesting to note that the synergic effect amplification rate (the slopes in Fig. 4a) along with the reduction in VOC emissions is nonlinearly modulated by the variation in NOx emissions, exhibiting first an enhanced trend (from 1.9 (green line in Fig. 4a) without NOx emission reduction to 3.4 (blue line in Fig. 4a) when half NOx emissions are reduced) and then a decrease. When episodic events are considered, although the general features are consistent with the monthly mean scale, the synergic effect is amplified even faster and to a greater extent with the reduction in anthropogenic VOC emissions.

The synergic effect of biogenic emissions tends to be larger during the ozone episodic events compared to the monthly scale. For instance, during the ozone episode of June 14–21 and June 26–30 (or June 2017), biogenic emissions contribute to 14.4 ppbv (or 10.2 ppbv) MDA8 ozone concentration over urban Beijing when all emissions are included, and biogenic emissions reaches a maximal contribution of 18.6 ppbv (or 12.0 ppbv) when anthropogenic VOCs are turned off (green line in Fig. 4a, c), corresponding to a maximum of 27% (Supplementary Fig. 4c) (or 20%, Supplementary Fig. 4a) of the contributions from anthropogenic emissions. In terms of the MDA8 ozone concentration

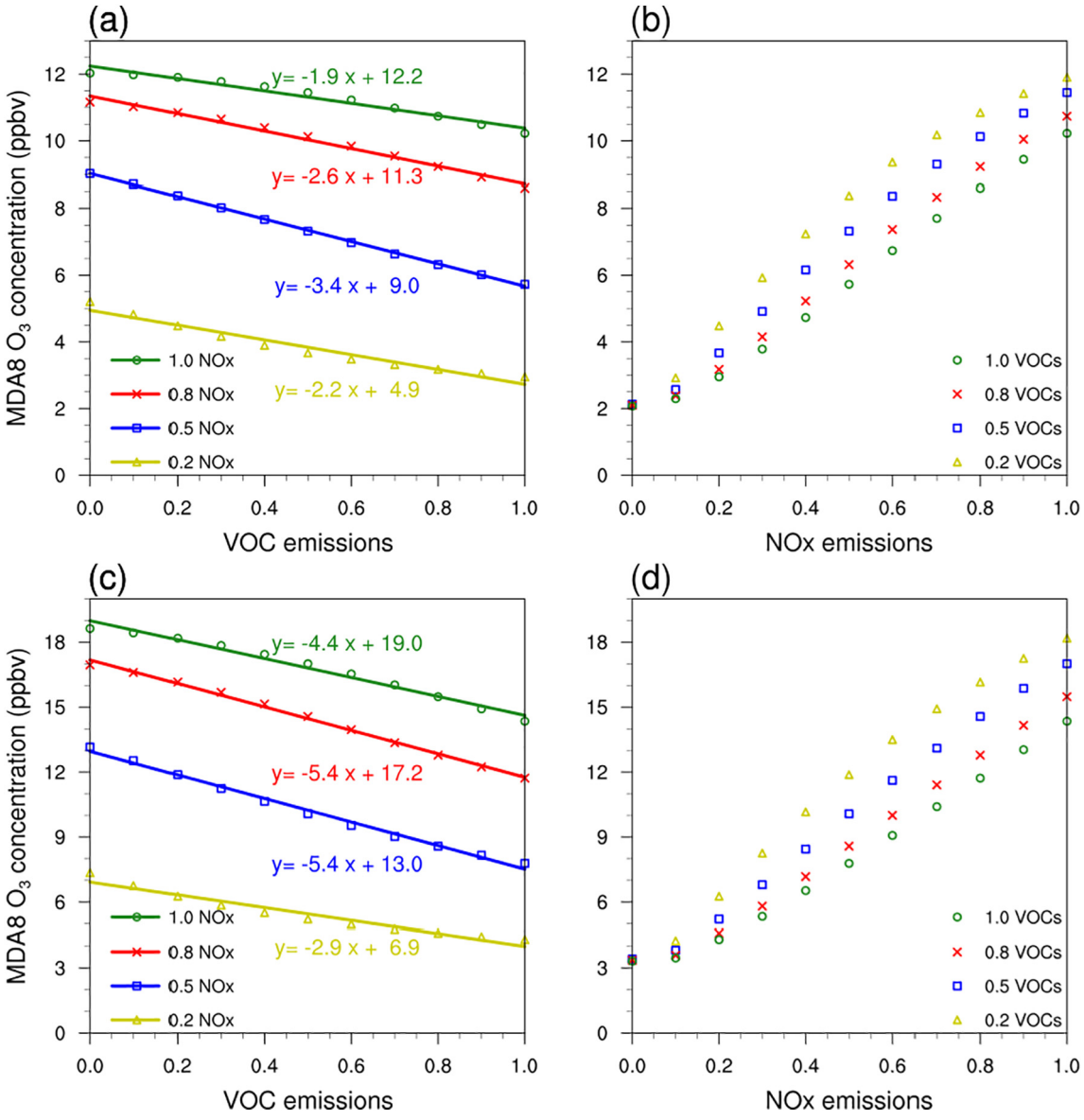

Fig. 4. The synergic effect of biogenic emissions on MDA8 ozone over urban Beijing. Shown are the contributions of biogenic emissions associated with the reduction of anthropogenic VOC (under fixed NOx; left column) or NOx (under fixed VOCs; right column) emissions in the month of June (top) and ozone episodic events (June 14–June 21, June 26–June 30; bottom). Please note the emission reduction is conducted over NCP. The numbers on the X axis indicate the ratio of changes in the anthropogenic emissions, with the value of 1.0 representing the case without the respective emission (VOCs or NOx) change and 0 meaning the emissions (VOCs or NOx) are zeroed out. All correlation coefficients of the linear regression (left column) are close to 1.0, showing statistical significance ($P < 0.05$).

over the entire NCP, whereas the amplification rate of the synergic effect with the reduction of anthropogenic VOC emissions still holds, the behavior associated with the NOx emissions differs, showing a monotonic decrease in the amplification rate when NOx emissions are reduced (left column in Supplementary Fig. 5), in contrast to the dipole pattern exhibited in the rate changes over urban Beijing (left column in Fig. 4).

The effect of transport on MDA8 ozone concentrations in Beijing is further examined by considering emission reductions over the entire domain (Supplementary Fig. 4b,d and Supplementary Fig. 6), which indicates a more enhanced synergic effect from biogenic emission reduction along with anthropogenic emission reduction. As an example, the episode (Supplementary Fig. 6c, d) shows that the MDA8 ozone concentration change rate may reach 8.2 ppbv (maximum) per 10% reduction in anthropogenic VOCs when the reduction is higher than 60%. For the same rate of emission reduction, the amplification rate of the synergic effect in urban Beijing is larger when the emission control is across the entire domain in comparison to the NCP. Specifically, biogenic emissions contribute to a maximum of 21.5 ppbv (Supplementary Fig. 6c) or 18.6 ppbv (Fig. 4c) when anthropogenic VOCs are eliminated over the entire domain or NCP, corresponding to a maximum of 36% (Supplementary Fig. 4d) or 27% (Supplementary Fig. 4c) of the contribution from anthropogenic emissions. Thus, there are vital implications that under a wide-area emission control scenario, regional transport may foster biogenic emissions with a further strengthened role in triggering the accumulation of ozone in megacities, as well as regions such as the NCP (Supplementary Figs. 5, 7).

When VOC emissions are unchanged, the synergic effect with the reduction in NOx emissions nevertheless reveals distinctive characteristics. The contributions of biogenic emissions to ozone concentrations display a predominant decrease as NOx emissions are reduced, tending to converge when NOx emissions are quite low (the leftmost markers in Fig. 4b, d). The feature of convergence leads to a nonlinear effect

characterized by a change in the weakening rate of the synergic effect associated with a reduction in NOx emissions. Overall, the diminished synergic effect concomitant with the reduction in NOx emissions is quite promising and can potentially be used in the quantification of controllable biogenically induced ozone. For instance, when all VOC emissions are included, the synergic effect is reduced from 10.2 ppbv (or 14.4 ppbv) to 2.1 ppbv (or 3.3 ppbv) over urban Beijing in June (or the ozone episode) along with the relative magnitude of NOx emissions from 1.0 (no reduction) to 0.0 (completed excluded), which implies that more than 70% of biogenically induced ozone concentrations may potentially be controlled therein (green markers in Fig. 4b, d).

Ozone, $PM_{2.5}$ and trace elements, are the leading air pollutants associated with human health effects (Kim et al., 2015; Wang et al., 2017; Zhang et al., 2020); therefore, ozone exceedance of national standards is of great interest to evaluate concerns from a health perspective. To achieve better statistics by utilizing a larger sample, all grids over the NCP in June 2017 are included in the analysis, and an MDA8 ozone concentration of 160 μg/m^3 (approximately 82 ppbv at 298 K, 1 atm.), based on the Chinese National Ambient Air Quality Standard (tier II), is used in the evaluation of ozone exceedance (Fig. 5).

When only anthropogenic emissions are considered (top row of Fig. 5), there is a total MDA8 ozone exceedance of 36% over NCP. Keeping the NOx emissions unchanged, the monotonic reduction (10% each step) in anthropogenic VOC emissions over NCP yields an almost linear decrease in ozone exceedance (1% per 10% VOC emission reduction; red bars in Fig. 5a). Under invariable VOC emissions (Fig. 5b), the reduction in NOx emissions over NCP corresponded to a comparable decrease in the ozone exceedance rate of 1%–2% per 10% emission reduction when the emission reduction is smaller than 40%; however, a higher rate at 3% to 5% may be achieved for the same emission change interval (10%) when the total NOx level reduction reaches 50% or more. The weaker change rate of ozone exceedance under high NOx conditions is primarily attributable to the titration effect. The response rate increase concomitant with the larger reduction in NOx emissions reveals that a larger benefit may be achievable upon continuous NOx emission control (red bars in Fig. 5b). The simultaneous reduction in both VOC and NOx emissions at the same rate leads to an even larger decrease in ozone exceedance compared to that seen when either the VOC or NOx emissions change alone (red bars in Fig. 5c vs. Fig. 5a, b). This is seemingly contradictory to what is displayed in Fig. 3a, in which the decrease in VOCs alone tends to be more effective than the same rate of reduction in both VOCs and NOx (cyan dots vs. black dots in Fig. 3a). This phenomenon can be understood from two perspectives. On the one hand, the NO titration effect in Fig. 3a is over urban Beijing, and the ozone exceedance discussed in Fig. 5 is over the region of NCP. As discussed earlier, the MDA8 ozone EKMA diagram based on NCP (Supplementary Fig. 1) infers much weaker titration effect than urban Beijing (Fig. 2). On the other hand, ozone exceedance is likely to be weighted

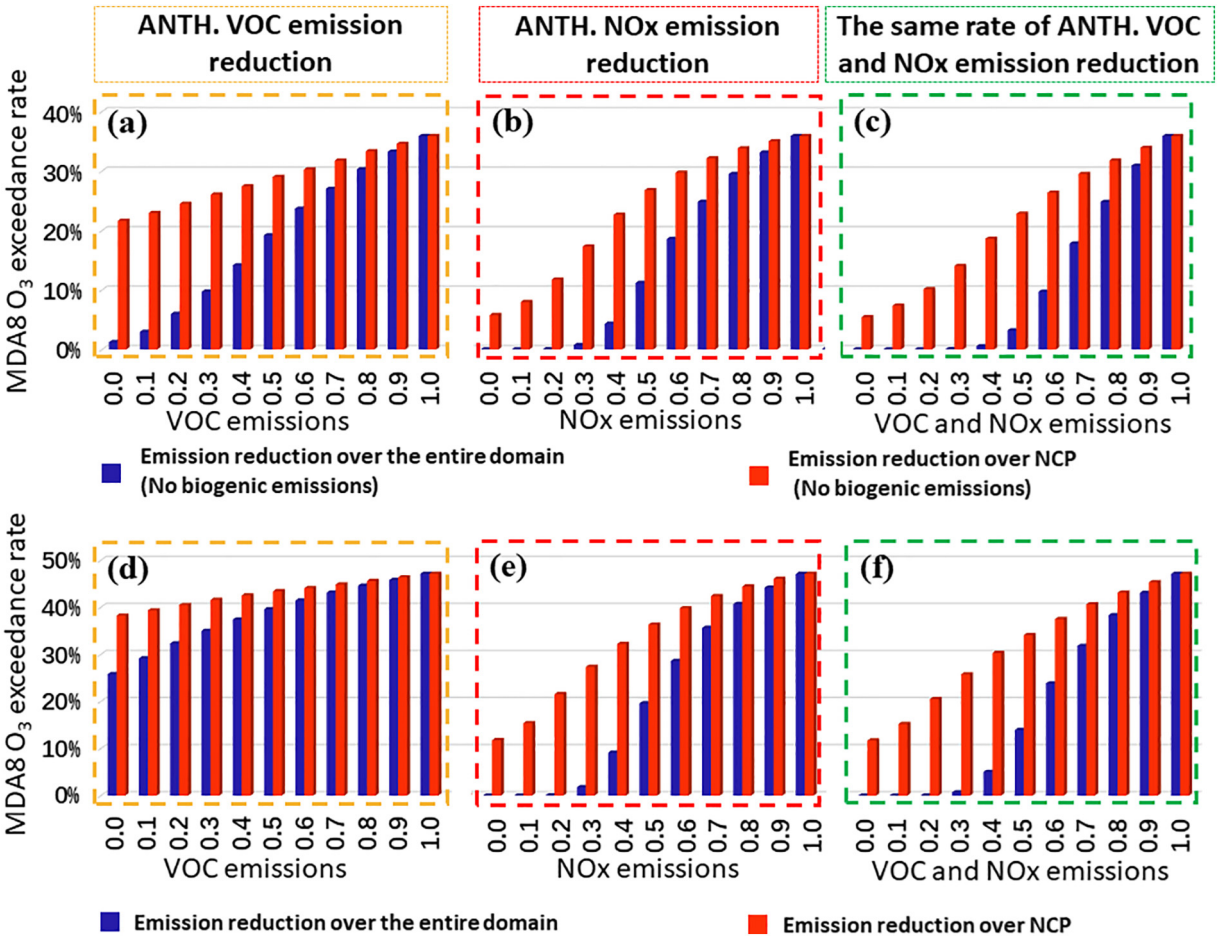

Fig. 5. The rate of MDA8 ozone exceedance of 82 ppbv. Shown are results over the NCP in June 2017 with anthropogenic emissions only (top) and with both anthropogenic and biogenic emissions (bottom), including emission reduction in the NCP (red bars) and the entire domain (blue bars). The numbers on the X axis indicate the ratio of changes in the anthropogenic emissions, with the value of 1.0 representing the case without the respective emission change, including anthropogenic VOC emissions (left column), NOx emissions (middle column) and the same rate (1:1 ratio) of VOC and NOx (right column) and 0.0 meaning the emissions (VOCs or NOx) are zeroed out.

toward higher ozone concentration days/areas, which in turn means it is less likely to be affected by the titration effect in view of the stronger photochemical reactions therein.

Another parallel set of numerical experiments is conducted with the only difference being that emission reduction is considered across the entire domain instead of only in the NCP, aiming to illustrate the effect of regional transport on MDA8 ozone exceedance in the NCP (blue bars in Fig. 5a–c). The results in general indicate that with the simultaneous emission reduction inside and outside of the NCP, the impact of transport, reflected by the differences between the red and blue bars in Fig. 5, becomes much larger, from ~1% at the beginning (i.e., emission reduction of 10%) to more than 15% when emission reduction reaches more than half. By reducing emissions of NOx alone or both VOCs and NOx, the transport (differences between the red and blue bars in Fig. 5b, c) yields a larger impact compared to that from the emissions over NCP (the difference of each red bar to the rightmost red bar in Fig. 5b, c). When only reducing VOCs (Fig. 5a), the NCP local emissions play a larger role than the transport at the beginning, but their impact is smaller once VOCs are reduced by more than 50%. This demonstrates the essential efficacy of mutual emission control on a broadly regional scale to better address the ozone exceedance issue.

When both anthropogenic and biogenic emissions are considered (bottom row of Fig. 5), an additional 11% (a total of 47%; rightmost red bar in Fig. 5d) of ozone exceedance in the NCP is induced relative to the scenario with anthropogenic emissions alone (36%; rightmost red bar in Fig. 5a). The comparison between the top and bottom rows in Fig. 5 illustrates that the influence of biogenic emissions on ozone exceedance overall delineates a dipole feature upon the changes in anthropogenic emissions; that is, it has a larger role when accompanied by the decrease in anthropogenic VOC emissions but a smaller effect when NOx emissions are reduced. This emphasizes the importance of NOx emission reduction in further weakening the influence of biogenic emissions on ozone exceedance. Specifically, when the anthropogenic VOC or NOx emissions inside the NCP are reduced (red bars in Fig. 5d vs. Fig. 5a, Fig. 5e vs. Fig. 5b), the maximal contributions of biogenic emissions to ozone exceedance over the NCP occurs during the 100% reduction of VOC or no reduction of NOx, with values of 17% or 11%, respectively. This effect is consistent with the preceding discussions of the amplified or weakened role in modulating the mean ozone concentration along with the reductions of anthropogenic VOCs or NOx emissions, respectively. In contrast, direct comparison of the impacts of anthropogenic and biogenic emissions on ozone exceedance reveals that biogenic emissions contribute to approximately one-third of ozone exceedance without emission reduction, while a gradual reduction in anthropogenic emissions, regardless of VOCs or NOx, leads to a uniformly enhanced contribution (%) in biogenic emissions relative to anthropogenic emissions, even yielding comparable or larger contributions from biogenic emissions than anthropogenic emissions.

When the ozone episode is considered (Supplementary Fig. 8), similar conclusions to those described above can be drawn, with the starting ozone exceedance rate higher (71%/57% in the episode vs. 47%/36% in June 2017; with/without biogenic emissions) during favorable meteorological conditions. When 70 ppbv is selected based on the National Ambient Air Quality Standards (NAAQS) set by the US Environmental Protection Agency (EPA) (Supplementary Fig. 9), the exceedance rate is approximately one-third higher than that based on 82 ppbv. In particular, the rate of exceedance to 70 ppbv during the ozone episode (Supplementary Fig. 10) may reach 83% or 78% with or without biogenic emissions, and even with all anthropogenic emissions eliminated over the NCP, there are still correspondingly 42% (with biogenic emissions) or 30% (without biogenic emissions) of the days with ozone exceedance.

To gain further insight into ozone exceedance under the SSP scenarios, linear interpolations are performed based on the ozone exceedance (Fig. 5) and the emission reduction rate (Supplementary Table 1) under the assumption of invariable meteorological conditions. The results are shown in Table 2. The MDA8 ozone exceedance generally decreases, consistent with the emission reductions in most of the SSPs. In 2060, if only NCP emissions are controlled, even under the quasi carbon neutrality scenario (SSP126), there is still 20% ozone exceedance of 82 ppbv and 44% ozone exceedance of 70 ppbv. When the emission reduction is carried out in a much larger area, there is almost no ozone exceedance of either 82 ppbv or 70 ppbv (only 1%). The results, on the one hand, illustrate the challenge in achieving substantially reduced ozone exceedance and, on the other hand, emphasize the importance of coordinated emission control on a large regional scale. More importantly, the role of biogenic emissions may be even more important than that of anthropogenic emissions in the context of irreversible anthropogenic emission reduction and the need for an increase in carbon sinks.

4. Conclusions and implications

This study describes the systematic investigation of the synergic effect of biogenic and anthropogenic emissions on MDA8 ozone concentrations and exceedance of two selected standards (82 ppbv and 70 ppbv). The synergic effect, primarily characterized as the effect of biogenic emissions on ozone concentrations along with changes in anthropogenic emissions, is nicely delineated in an EKMA diagram, mimicking the O_3-NOx-VOC relationship and revealing distinct interactions between biogenic and anthropogenic emissions. The synergic effect on both ozone concentrations and exceedance is generally amplified concomitant with the reduction of anthropogenic VOC emissions but diminished in response to NOx emissions.

The effect of carbon neutrality is also examined under the assumption of invariable meteorological conditions. Based on the EKMA diagram based on the numerical experiments, we find that the emission reduction in the projected SSPs is crucial in alleviating ozone pollution, quantified based on MDA8 ozone concentrations and exceedance. Specifically, the carbon neutrality in 2060 corresponds to a high emission reduction (91% VOCs, 81% NOx relative to 2015 in SSP 126), triggering

Table 2
The MDA8 ozone exceedance rate (%).

		Emission reduction over the NCP					Emission reduction over the entire domain				
		Year									
MDA8 O_3 exceedance of 82 ppbv (%)	SSPs	2020	2030	2040	2050	2060	2020	2030	2040	2050	2060
	SSP119	44	33	25	20	15	41	11	0	0	0
	SSP126	44	39	33	25	20	41	27	9	0	0
	SSP245	47	46	40	34	29	46	44	29	13	4
	SSP585	46	44	44	44	41	44	40	40	39	33
		Year									
MDA8 O_3 exceedance of 70 ppbv (%)	SSPs	2020	2030	2040	2050	2060	2020	2030	2040	2050	2060
	SSP119	65	58	50	44	36	63	40	13	1	0
	SSP126	65	62	58	49	44	63	53	38	12	1
	SSP245	66	65	64	60	54	66	64	55	40	23
	SSP585	66	66	66	65	64	65	63	62	62	58

a large alleviation of ozone pollution. Nevertheless, climate change may project more frequent extreme weather events including heat waves, stagnation and drought

(Gao et al., 2012; Gao et al., 2014; Zhang et al., 2018a), which could represent a strong challenge in ozone pollution control under a warming climate. Global warming and the potential increase in vegetation due to the urgent need for carbon sink enhancement may unavoidably trigger an increase in biogenic emissions, which may substantially reinforce the synergistic effect and pose a high challenge in ozone air quality improvement. The main findings in this study are based on the simulations of June 2017; nevertheless, the conclusions should be robustly applicable to other periods when ozone is a concern.

CRediT authorship contribution statement

Yang Gao: Conceptualization, Methodology, Formal analysis, Writing – original draft. **Feifan Yan:** Formal analysis, Writing – review & editing. **Mingchen Ma:** Validation. **Aijun Ding:** Visualization, Writing – review & editing. **Hong Liao:** Writing – review & editing. **Shuxiao Wang:** Visualization, Writing – review & editing. **Xuemei Wang:** Visualization, Writing – review & editing. **Bin Zhao:** Writing – review & editing. **Wenju Cai:** Writing – review & editing. **Hang Su:** Writing – review & editing. **Xiaohong Yao:** Writing – review & editing. **Huiwang Gao:** Writing – review & editing.

Declaration of competing interest

The authors declare that they have no known competing financial interests or personal relationships that could have appeared to influence the work reported in this paper.

Acknowledgement

This research was supported by grants from the National Natural Science Foundation of China (42122039, 21625701) and Fundamental Research Funds for the Central Universities (201941006). The analysis was performed using the computing resources of Center for High Performance Computing and System Simulation, Pilot National Laboratory for Marine Science and Technology (Qingdao).

Appendix A. Supplementary data

Supplementary data to this article can be found online at https://doi.org/10.1016/j.scitotenv.2021.151722.

References

Cai, B., Cao, L., Lei, Y., Wang, C., Zhang, L., Zhu, J., et al., 2021. China's carbon emission pathway under the carbon neutrality target. China Popul.Resour. Environ. 31, 25–32.
Carlton, A.G., Pinder, R.W., Bhave, P.V., Pouliot, G.A., 2010. To what extent can biogenic SOA be controlled? Environ. Sci. Technol. 44, 3376–3380.
Chen, X., Situ, S.P., Zhang, Q., Wang, X.M., Sha, C.Y., Zhouc, L.Y., et al., 2019. The synergetic control of NO2 and O-3 concentrations in a manufacturing city of southern China. Atmos. Environ. 201, 402–416.
Cheng, J., Tong, D., Zhang, Q., Liu, Y., Lei, Y., Yan, G., et al., 2021. Pathways of China's PM2.5 air quality 2015–2060 in the context of carbon neutrality. Natl. Sci. Rev. 0, 1–11.
Emmons, L.K., Walters, S., Hess, P.G., Lamarque, J.F., Pfister, G.G., Fillmore, D., et al., 2010. Description and evaluation of the model for ozone and related chemical tracers, version 4 (MOZART-4). Geosci. Model Dev. 3, 43–67.
Gao, Y., Fu, J.S., Drake, J.B., Liu, Y., Lamarque, J.-F., 2012. Projected changes of extreme weather events in the eastern United States based on a high-resolution climate modeling system. Environ. Res. Lett. 7, 044025.
Gao, Y., Fu, J.S., Drake, J.B., Lamarque, J.F., Liu, Y., 2013. The impact of emission and climate change on ozone in the United States under representative concentration pathways (RCPs). Atmos. Chem. Phys. 13, 9607–9621.
Gao, Y., Leung, L.R., Lu, J., Liu, Y., Huang, M., Qian, Y., 2014. Robust spring drying in the southwestern U.S. And seasonal migration of wet/dry patterns in a warmer climate. Geophys. Res. Lett. 41, 1745–1751.
Gao, Y., Shan, H.Y., Zhang, S.Q., Sheng, L.F., Li, J.P., Zhang, J.X., et al., 2020a. Characteristics and sources of PM2.5 with focus on two severe pollution events in a coastal city of Qingdao, China. Chemosphere 247, 8.
Gao, Y., Zhang, J.X., Yan, F.F., Leung, L.R., Luo, K., Zhang, Y., et al., 2020b. Nonlinear effect of compound extreme weather events on ozone formation over the United States. Weather Clim. Extremes 30, 13.
Gidden, M.J., Riahi, K., Smith, S.J., Fujimori, S., Luderer, G., Kriegler, E., et al., 2019. Global emissions pathways under different socioeconomic scenarios for use in CMIP6: a dataset of harmonized emissions trajectories through the end of the century. Geosci. Model Dev. 12, 1443–1475.
Kim, Y.M., Zhou, Y., Gao, Y., Fu, J.S., Johnson, B.A., Huang, C., et al., 2015. Spatially resolved estimation of ozone-related mortality in the United States under two representative concentration pathways (RCPs) and their uncertainty. Clim. Chang. 128, 71–84.
Kriegler, E., O'Neill, B.C., Hallegatte, S., Kram, T., Lempert, R.J., Moss, R.H., et al., 2012. The need for and use of socio-economic scenarios for climate change analysis: a new approach based on shared socio-economic pathways. Glob. Environ. Change. 22, 807–822.
Li, N., He, Q., Greenberg, J., Guenther, A., Li, J., Cao, J., et al., 2018. Impacts of biogenic and anthropogenic emissions on summertime ozone formation in the Guanzhong BasinChina. Atmos. Chem. Phys. 18, 7489–7507.
Li, K., Jacob, D.J., Liao, H., Shen, L., Zhang, Q., Bates, K.H., 2019. Anthropogenic drivers of 2013–2017 trends in summer surface ozone in China. Proc. Natl. Acad. Sci. U. S. A. 116, 422–427.
Lu, X., Zhang, L., Chen, Y.F., Zhou, M., Zheng, B., Li, K., et al., 2019. Exploring 2016–2017 surface ozone pollution over China: source contributions and meteorological influences. Atmos. Chem. Phys. 19, 8339–8361.
Ma, M.C., Gao, Y., Wang, Y.H., Zhang, S.Q., Leung, L.R., Liu, C., et al., 2019. Substantial ozone enhancement over the North China Plain from increased biogenic emissions due to heat waves and land cover in summer 2017. Atmos. Chem. Phys. 19, 12195–12207.
Ou, J.M., Yuan, Z.B., Zheng, J.Y., Huang, Z.J., Shao, M., Li, Z.K., et al., 2016. Ambient ozone control in a photochemically active region: short term despiking or long-term attainment? Environ. Sci. Technol. 50, 5720–5728.
Rao, S., Klimont, Z., Smith, S.J., Van Dingenen, R., Dentener, F., Bouwman, L., et al., 2017. Future air pollution in the shared socio-economic pathways. Glob. Environ. Change-Human Policy Dimens. 42, 346–358.
Riahi, K., van Vuuren, D.P., Kriegler, E., Edmonds, J., O'Neill, B.C., Fujimori, S., et al., 2017. The shared socioeconomic pathways and their energy, land use, and greenhouse gas emissions implications: an overview. Glob. Environ. Change-Human Policy Dimens. 42, 153–168.
Romer, P.S., Duffey, K.C., Wooldridge, P.J., Edgerton, E., Baumann, K., Feiner, P.A., et al., 2018. Effects of temperature-dependent NOx emissions on continental ozone production. Atmos. Chem. Phys. 18, 2601–2614.
Saha, S., Moorthi, S., Wu, X.R., Wang, J., Nadiga, S., Tripp, P., et al., 2014. The NCEP climate forecast system version 2. J. Clim. 27, 2185–2208.
Shen, F.Z., Zhang, L., Jiang, L., Tang, M.Q., Gai, X.Y., Chen, M.D., et al., 2020. Temporal variations of six ambient criteria air pollutants from 2015 to 2018, their spatial distributions, health risks and relationships with socioeconomic factors during 2018 in China. Environ. Int. 137, 13.
Sillman, S., 1999. The relation between ozone, NOx and hydrocarbons in urban and polluted rural environments. Atmos. Environ. 33, 1821–1845.
Sillman, S., He, D.Y., 2002. Some theoretical results concerning O-3-NOx-VOC chemistry and NOx-VOC indicators. J. Geophys. Res.-Atmos. 107, 15.
Stein, U., Alpert, P., 1993. Factor separation in numerical simulations. J. Atmos. Sci. 50, 2107–2115.
Tao, Z.N., Larson, S.M., Wuebbles, D.J., Williams, A., Caughey, M., 2003. A summer simulation of biogenic contributions to ground-level ozone over the continental United States. J. Geophys. Res.-Atmos. 108.
van Vuuren, D.P., Edmonds, J., Kainuma, M., Riahi, K., Thomson, A., Hibbard, K., et al., 2011. The representative concentration pathways: an overview. Clim. Chang. 109, 5–31.
Wang, J.D., Xing, J., Mathur, R., Pleim, J.E., Wang, S.X., Hogrefe, C., et al., 2017. Historical trends in PM2.5-related premature mortality during 1990–2010 across the Northern Hemisphere. Environ. Health Perspect. 125, 400–408.
Wang, W.N., Ronald, V., Ding, J.Y., van Weele, M., Cheng, T.H., 2021. Spatial and temporal changes of the ozone sensitivity in China based on satellite and ground-based observations. Atmos. Chem. Phys. 21, 7253–7269.
Wu, K., Yang, X.Y., Chen, D., Gu, S., Lu, Y.Q., Jiang, Q., et al., 2020. Estimation of biogenic VOC emissions and their corresponding impact on ozone and secondary organic aerosol formation in China. Atmos. Res. 231, 11.
Xu, L., Guo, H.Y., Boyd, C.M., Klein, M., Bougiatioti, A., Cerully, K.M., et al., 2015. Effects of anthropogenic emissions on aerosol formation from isoprene and monoterpenes in the southeastern United States. Proc. Natl. Acad. Sci. U. S. A. 112, 37–42.
Yan, F.F., Gao, Y., Ma, M.C., Liu, C., Ji, X.G., Zhao, F., et al., 2021. Revealing the modulation of boundary conditions and governing processes on ozone formation over northern China in June 2017. Environ. Pollut. 272, 12.
Zhang, J., Gao, Y., Luo, K., Leung, L.R., Zhang, Y., Wang, K., et al., 2018a. Impacts of compound extreme weather events on ozone in the present and future. Atmos. Chem. Phys. 18, 9861–9877.
Zhang, J.X., Gao, Y., Luo, K., Leung, L.R., Zhang, Y., Wang, K., et al., 2018b. Impacts of compound extreme weather events on ozone in the present and future. Atmos. Chem. Phys. 18, 9861–9877.
Zhang, L., Gao, Y., Wu, S.L., Zhang, S.Q., Smith, K.R., Yao, X.H., et al., 2020. Global impact of atmospheric arsenic on health risk: 2005 to 2015. Proc. Natl. Acad. Sci. U. S. A. 117, 13975–13982.